Neuron, Vol. 42, 897–912, June 24, 2004, Copyright ©2004 by Cell Press

NGF-Induced Axon Growth Is Mediated by Localized Inactivation of GSK-3β and Functions of the Microtubule Plus End Binding Protein APC

Feng-Quan Zhou,[1] Jiang Zhou,[1] Shoukat Dedhar,[2] Yao-Hong Wu,[1] and William D. Snider[1,*]
[1]UNC-Neuroscience Center
University of North Carolina at Chapel Hill
Chapel Hill, North Carolina 27599
[2]BC Cancer Agency
Jack Bell Research Centre
Vancouver, British Columbia V6H 3Z6
Canada

Summary

Little is known about how nerve growth factor (NGF) signaling controls the regulated assembly of microtubules that underlies axon growth. Here we demonstrate that a tightly regulated and localized activation of phosphatidylinositol 3-kinase (PI3K) at the growth cone is essential for rapid axon growth induced by NGF. This spatially activated PI3K signaling is conveyed downstream through a localized inactivation of glycogen synthase kinase 3β (GSK-3β). These two spatially coupled kinases control axon growth via regulation of a microtubule plus end binding protein, adenomatous polyposis coli (APC). Our results demonstrate that NGF signals are transduced to the axon cytoskeleton via activation of a conserved cell polarity signaling pathway.

Introduction

Axon morphogenesis, including outgrowth, guidance, and preterminal branching, is carefully orchestrated during embryonic development to establish the correct wiring of the nervous system. Signaling pathways mediating these events must ultimately converge to regulate the reorganization of the neuronal cytoskeleton. However, we still know relatively little about the linkage between the major signaling pathways that mediate axon growth and the underlying cytoskeletal mechanisms.

A variety of extracellular cues, including intermediate- and long-range target-derived factors, contribute to regulating axon morphologies. One such group of molecules, key to the development of the axon projections of neurons in the peripheral nervous system (PNS), are the neurotrophins. By binding to their specific receptor tyrosine kinases (TRKs), neurotrophins strongly activate both the MAPK and PI3K pathways in neurons (see Segal, 2003, for a recent review). Coordinated action of these pathways mediates the biological effects of neurotrophins on survival and axon growth. Neurotrophin-stimulated axon outgrowth requires the activation of transcription factors and continuous gene expression and protein synthesis to supply raw materials for axon growth (see Markus et al., 2002a, for a review). In addition to gene expression, a local signaling pathway activated by neurotrophins is required to control the assembly of cytoskeletal proteins into axons. The importance of such local signaling was established by studies more than two decades ago in which neuron cell bodies were separated from their axons (Campenot, 1982a, 1982b). These "Campenot Chamber" studies demonstrated that NGF-activated gene expression in the cell bodies alone was not sufficient to support axon growth into the side compartment. The presence of NGF in the axon compartment is absolutely required. Despite the fact that neurotrophin signaling has been the subject of numerous investigations during the past two decades, surprisingly little is known about how this local signaling regulates the cytoskeleton to form the axon.

There is mounting evidence that PI3K is involved in local signaling underlying several aspects of neurotrophin-mediated axon morphogenesis, including elongation and guidance. Thus, pharmacological studies in compartmentalized cultures have established that PI3K signaling is required for axon growth into an NGF-containing side chamber (Atwal et al., 2000). Experimental evidence also implicates local PI3K signaling in mediating the turning and branching effects of neurotrophins applied locally at the growth cone or axon shaft (Gallo and Letourneau, 1998; Ming et al., 1999). A number of signaling molecules, such as Akt, integrin-linked kinase (ILK), and GSK-3β, with potential to regulate the cytoskeleton are established as downstream mediators of PI3K in neurons and nonneuronal cells (reviewed by Cantley, 2002). Furthermore, in nonneuronal cells, it is well established that PI3K signaling regulates actin dynamics through the regulation of Rac (Reif et al., 1996). To date, however, the mechanisms by which PI3K regulates axon elongation are unclear.

Growth cones at the tips of growing axons are the major sites where neurons receive and integrate extracellular signals to direct axonal cytoskeletal assembly (see Baas and Luo, 2001, for a review). Axon elongation is initiated with growth cone advancement via actin polymerization at the leading edge. Subsequent microtubule polymerization and bundling are the major events that mediate the formation of axons (Gordon-Weeks, 1991). Although the cytoskeletal mechanisms underlying growth cone motility during axon growth and guidance have been extensively studied, how extracellular signals control the growth cone cytoskeleton, especially the microtubules, remains a significant question (see Dent and Gertler, 2003, for a review).

A signaling mediator downstream of PI3K that could lead to microtubule regulation is GSK-3β (Mills et al., 2003). GSK-3β, first identified as a regulator of glycogen synthesis, is now known to be involved in the signaling pathways of insulin and growth factors acting through receptor tyrosine kinases. It is constitutively active in resting cells and must be inactivated by extracellular signals to allow the activation of its substrates (see Woodgett, 2001, and Cohen and Frame, 2001, for reviews). In neuronal cells, GSK-3β is inactivated by PI3K-mediated phosphorylation and has been shown to affect PI3K-mediated neuronal survival (Crowder and Freeman, 2000; Hetman et al., 2000). GSK-3β has also been

*Correspondence: william_snider@med.unc.edu

intensively studied because of its key role in Wnt signaling. In the Wnt pathway, GSK-3β forms a complex with axin and APC, phosphorylates these substrates, and controls gene expression by regulating β-catenin levels (see Woodgett, 2001, for a review). In addition to the regulation of β-catenin levels in the Wnt pathway, APC has recently been shown in nonneuronal cells to bind to the plus ends of microtubules and stabilize their growing ends, a property that is abolished by GSK-3β phosphorylation (Zumbrunn et al., 2001). APC binds to microtubules with its C terminus, either directly via the basic domain or indirectly via the EB1 binding domain (Mimori-Kiyosue and Tsukita, 2001). Recent studies have demonstrated the role of GSK-3β-APC-microtubule interactions in regulating polarized cell migration downstream of the cdc42-par3/par6 pathway (Etienne-Manneville and Hall, 2003). It would be interesting to test whether this pathway plays a role in axon outgrowth, another well-known example of cell polarization involving microtubule reorganization. Indeed, APC is highly enriched in the nervous system of both vertebrates and invertebrates (Akong et al., 2002; Bhat et al., 1994; Brakeman et al., 1999).

In the present studies, we demonstrate that a tightly regulated and localized activation of PI3K at the growth cone is essential for rapid axon growth induced by NGF. This spatially activated PI3K signaling is conveyed downstream through a localized inactivation of GSK-3β. We further show that these two spatially coupled kinases control axon growth by regulating a microtubule plus end binding protein, APC. Our findings provide evidence that spatially controlled signal transduction is necessary for efficient axon elongation. Moreover, we define a signaling cascade from an extracellular signal to the growth cone cytoskeleton. Last, we demonstrate that an evolutionarily conserved pathway regulating cell polarity also controls axon elongation induced by neurotrophins.

Results

A Spatially Regulated PI3K-GSK-3β Pathway at the Distal Axon Is Required for Rapid Axon Elongation

A previous study using a dominant inhibitory PI3K construct demonstrated that PI3K is a key signaling mediator that mediates NGF-induced axon growth (Markus et al., 2002b). To study the mechanism of this PI3K regulation, we first examined the localization of PI3K activation during NGF-mediated axon growth from embryonic mouse DRG neurons. Phosphorylated Akt was used as a marker for PI3K activation (see Shi et al., 2003). Our results showed localized staining of phospho-Akt at the distal ends of the axons (Figure 1A1), demonstrating a spatial distribution of activated PI3K. High-magnification imaging showed colocaliation of phospho-Akt with actin filaments in the growth cone (Figure 1A2). Quantitation of relative average fluorescence intensity along the axon normalized for the difference in total protein along the axon due to variations in axonal volume (see Experimental Procedures) verified that phospho-Akt staining was significantly higher at the growth cone than along the axon shaft (Figure 1B).

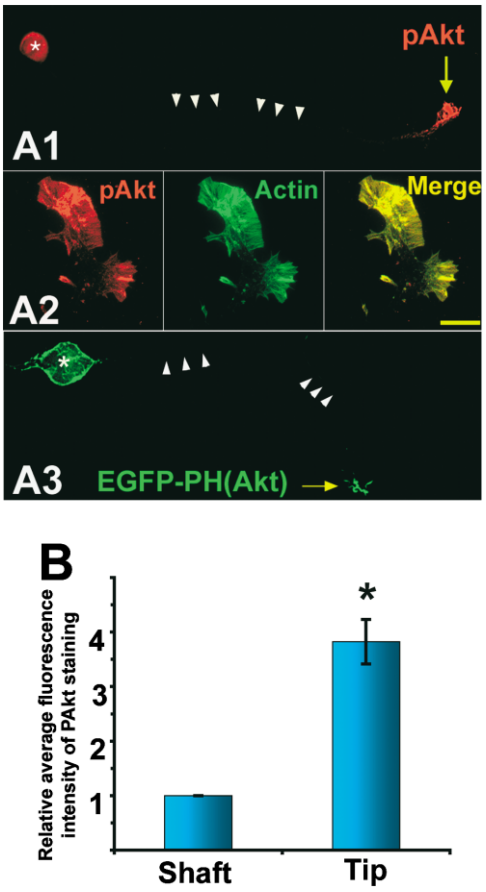

Figure 1. Spatially Regulated PI3K Activation at the Distal Axon

(A) Activation of PI3K in fixed neurons was indicated by staining for phosphorylated Akt (A1). pAkt was mainly found in the cell body (star) and the distal tip of the axon (the growth cone, yellow arrow). Little pAkt was detected along the axon shaft (white arrowheads). High magnification showed colocalization of pAkt with actin filaments (A2). Membrane accumulation of EGFP-PH-Akt was used as another indicator of PI3K activation (A3). EGFP-PH was localized primarily in the cell body (star) and the growth cone (yellow arrow). White arrowheads mark the axon shaft. Scale bar, 10 μm in (A2) and 30 μm in (A1) and (A3).

(B) Quantification of phospho-Akt staining at axon tip versus axon shaft. The value is expressed as a ratio of pAkt staining normalized to DTAF staining as a marker for total protein at the two locations. * Indicates significant difference from the axon shaft staining ($n = 3$ independent experiments, $p < 0.01$).

To visualize PI3K activation in real time, we transfected neurons with a construct encoding the PH domain derived from Akt coupled with EGFP. Upon PI3K activation, PH domain-containing proteins are recruited to the membrane by PIP3, the lipid product of PI3K (see Cantley, 2002, for a review). As shown in Figure 1A3, EGFP-PH (Akt) was highly concentrated at the leading edge of the growth cone (arrow), whereas little was found along the axon shaft (arrowheads). This result indicates spatially localized production of PIP3 at the growth cones. Time-lapse imaging showed sustained accumulation of EGFP-PH at the growth cone during axon extension (data not shown).

To test whether localized activation of PI3K is necessary for axon growth induced by NGF, we overexpressed

a constitutively activated PI3K in the form of the membrane-targeted chimeric protein p110-CAAX that localized along the entire axon. Control neurons expressing EGFP showed no changes in axon extension (Supplemental Figure S1A, top panel, arrows [available at http://www.neuron.org/cgi/content/full/42/6/897/DC1). In contrast, transfection with p110-CAAX resulted in a very significant retardation of axon elongation compared to control cells expressing EGFP (Supplemental Figures S1A, lower panel, and S1B). The inhibitory effect of p110-CAAX on axon growth was unlikely due to the nonspecific effect of the CAAX motif. In our hands, EGFP-CAAX has no effect on axon growth compared to EGFP alone (A. Markus and W.D.S., unpublished data). Furthermore, Raf-CAAX strongly promotes rather than inhibits axon growth in this same paradigm (Markus et al., 2002b). Taken together, these results suggest that localized activation of PI3K at the distal axon is important for efficient axon elongation induced by NGF.

A downstream target of PI3K with potential to regulate microtubules is GSK-3β. To test whether PI3K regulates GSK-3β activity in E-13 mouse DRG neurons, we detected GSK-3β phosphorylation by Western blotting. GSK-3β is constitutively active in resting cells. Upon growth factor stimulation, it is inactivated via phosphorylation of its serine 9 residue (Sutherland et al., 1993). Addition of the PI3K inhibitor LY294002 to DRG neurons in the presence of NGF reduced phosphorylation of GSK-3β at ser9 in a dose-dependent manner (Figure 2A). Addition of a different PI3K inhibitor, wortmannin, also led to a reduction in GSK-3β phosphorylation. These results are consistent with findings from a previous study using embryonic chicken DRG neurons (Eickholt et al., 2002). Specificity of these results was demonstrated by the fact that inhibition of ERK with inhibitor U0126 had no effect (data not shown). A decrease in GSK-3β phosphorylation was also seen after anti-NGF antibody treatment (data not shown). Moreover, readdition of NGF to NGF-starved DRG cultures induced dramatic increases in GSK-3β phosphorylation. This increase was antagonized by pretreatment of cells with LY294002 (Figure 2B). Together, these data demonstrate that NGF regulates GSK-3β activity via PI3K in embryonic mouse DRG neurons.

Downstream of PI3K, several kinases are candidates for mediating the phosphorylation of GSK-3β, including Akt (Cross et al., 1995), ILK (Mills et al., 2003), and PKC (Kanzaki et al., 2004). In PC12 cells, it has been shown that ILK phosphorylates GSK-3β downstream of NGF and PI3K. Furthermore, ILK localizes to growth cones and is required for NGF-induced axon growth from DRG neurons (Mills et al., 2003). We therefore investigated the role of ILK in mediating NGF-induced phosphorylation of GSK-3β in DRG neurons. Addition of a specific ILK inhibitor significantly blocked GSK-3β phosphorylation (Figure 2C), indicating that ILK acts downstream of PI3K in embryonic mouse DRG neurons to regulate GSK-3β activity.

We next examined the spatial distribution of GSK-3β activity by staining axons with an antibody recognizing ser9 phosphorylated GSK-3β. The result showed that phospho-GSK-3β (inactive GSK-3β) was concentrated at the distal end of the axon (Figure 2D), spatially well correlated with phospho-Akt (representing active PI3K) distribution. Quantitation showed that inactivated GSK-3β at the growth cone was significantly higher than in the axon shaft (Supplemental Figure S1C at http://www.neuron.org/cgi/content/full/42/6/897/DC1). Higher-magnification imaging revealed inactivated GSK-3β in the microtubule-rich central domain of the growth cone and colocalization of inactivated GSK-3β with actin filaments in the peripheral domain (Figure 2D). Similar colocalization with actin has been reported in growth cones of chicken DRG neurons (Eickholt et al., 2002) and at the leading edge of migrating astrocytes (Etienne-Manneville and Hall, 2003).

To show that this localized inactivation of GSK-3β is required for axon elongation induced by NGF, we overexpressed a GSK-3β mutant that cannot be inactivated by phosphorylation (GSK-3β S9A). Neurons expressing the mutant GSK-3β had significantly shorter axons than control neurons expressing EGFP (Figure 2F), indicating that GSK-3β must be inactivated to allow efficient axon elongation. However, inactivation of GSK-3β with a kinase inhibitor or via activation of Wnt signaling has also been shown to inhibit neurotrophin-induced axon extension (Krylova et al., 2002), suggesting that uniform inactivation of GSK-3β also impedes efficient axon elongation. To further test this idea, we transfected neurons with a construct encoding Frequently Rearranged in Advanced T cell Lymphomas 1 (Frat-1). Frat-1 is an endogenous GSK-3β inhibitor that blocks GSK-3β activity toward selected targets in the Wnt pathway, such as axin, APC, and β-catenin (Thomas et al., 1999). Immunostaining showed that the expressed Frat-1 was evenly distributed along the whole axon shaft, suggesting uniform interaction between Frat-1 and GSK-3β along the length of the axon (Figure 2E). Neurons expressing Frat-1 had much shorter axons compared with EGFP-expressing neurons (Figure 2F). Interestingly, Frat-1 expression also led to a 2.6-fold increase in the axon branching frequency (EGFP, $5.0 \pm 0.31 \times 10^{-3}$ branch points/μm; Frat-1, $13.4 \pm 0.38 \times 10^{-3}$ branch points/μm, $p < 0.0001$). Together, these results indicate that inactivation of GSK-3β is important for efficient axon elongation and that GSK-3β inactivation must be spatially localized to the distal axon and the growth cone.

NGF Regulates Microtubule Levels at the Distal Axon via the PI3K-GSK-3β Pathway

The results from the preceding sections suggest that the PI3K-GSK-3β pathway mediates NGF-induced axon growth. This mediation of axon growth presumably involves the regulation of axonal microtubules. To directly visualize microtubule polymers in axons, we extracted and fixed the neurons at the same time to eliminate tubulin monomers (as described by He et al., 2002) and then stained for polymerized microtubules. Under control conditions, in the presence of NGF, polymerized microtubules showed a distribution gradient along the axon, with higher density at the distal end (Figure 3A1). Treatment of neurons with the microtubule-stabilizing drug taxol markedly increased the density of polymerized microtubules in the distal region as expected (Figure 3A2). In contrast, the microtubule depolymerizing drug nocodozole almost eliminated polymerized micro-

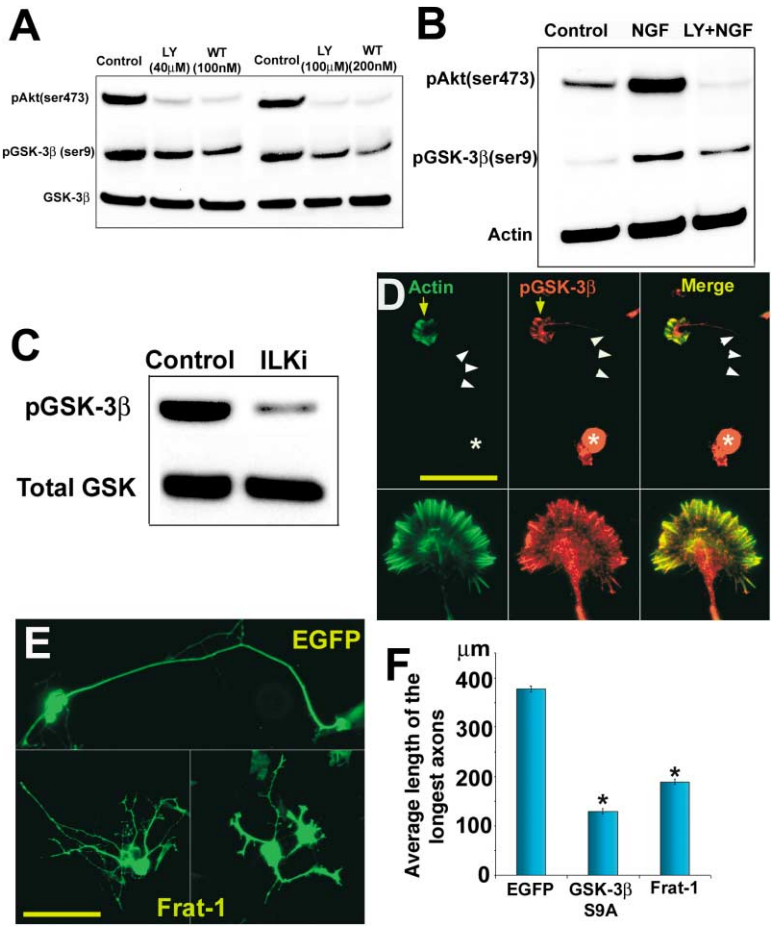

Figure 2. Regulation of GSK-3β by the NGF-PI3K Pathway

(A) Western blot analysis showed that GSK-3β was regulated by PI3K in cultures of E-13 DRG neurons. Treatment of neurons with either LY294002 or wortmannin decreased the amount of phosphorylated GSK-3β in a dose-dependent manner. Similar results were obtained in each of three independent experiments.

(B) Readdition of NGF to NGF-starved cultures markedly increased the phosphorylation of GSK-3β. This effect was antagonized by pretreatment with LY294002. A similar result was obtained in each of three independent experiments.

(C) Treatment of neurons with a specific ILK inhibitor, KP-074728 (ILKi), markedly decreased the phosphorylation of GSK-3β. Similar results were obtained in each of four independent experiments.

(D) Similar to phospho-Akt, phosphorylated GSK-3β was concentrated at the cell body (stars) and the distal end of the axon (yellow arrows), while little was detected along the axon shaft (white arrowheads). High-magnification images of the growth cone (bottom panel) showed colocalization of pGSK-3β with actin. The scale bar represents 50 μm in the top panel and 10 μm in the bottom panel.

(E) Overexpression of GSK-3β inhibiting protein Frat-1 blocked NGF-mediated axon growth. Scale bar, 100 μm.

(F) Quantification of the axon growth defect in neurons expressing the active GSK-3β mutant GSK-3β(S9A) and the GSK-3β inhibitor Frat-1 compared to control neurons expressing EGFP (40 to 80 neurons in each of 3 to 6 independent experiments were analyzed in each condition). * Indicates significant difference from the control ($p < 0.0001$).

tubules, especially at the axon distal ends (Figure 3A3). Therefore, this fix/extraction technique is able to detect changes in microtubule levels.

Using this method, we next asked how inhibition of NGF signaling affects microtubule levels in the axons. Treatment with an anti-NGF antibody significantly reduced the density of polymerized microtubules at the distal ends (Figure 3A5). A similar reduction in microtubule levels was observed in neurons treated with the PI3K inhibitor LY294002 (Figure 3A7), indicating the regulatory role of the NGF-PI3K pathway in axonal microtubules. As a control, neurons were also treated with jasplakinolide, an F-actin stabilizer that has been shown to cause axon retraction via increased actomyosin interaction without significant microtubule depolymerization (Gallo et al., 2002). In contrast to anti-NGF- or LY294002-treated neurons, retracted axons of these neurons exhibited high microtubule density at their distal ends (Figure 3A4). We next examined whether GSK-3β was involved in mediating NGF-PI3K regulation of microtubules. Neurons treated with a specific GSK-3β inhibitor (GSK-3β inhibitor I) were sensitive to neither anti-NGF treatment nor PI3K inhibition in terms of microtubule levels. They contained even higher microtubule density at their distal ends than that of control axons (Figures 3A6 and 3A8), which was consistent with the result that GSK-3β inhibitor treatment alone increased the distal microtubule level. These results suggest that inhibition of GSK-3β activity positively regulates microtubule levels downstream of the NGF-PI3K pathway. Quantitation of microtubule levels confirmed highly-significant effects of the NGF-PI3K-GSK-3β pathway in regulating axonal microtubules (Figure 3B).

In the axons of control NGF-stimulated neurons, axon branching rarely occurs along the axon shaft (Figure 3C). In contrast, treatment of the axon with GSK-3β inhibitors induced axon branching along the entire axon shaft (Figure 3C), indicating de novo microtubule assembly. This result suggests that GSK-3β inhibition plays an important role in promoting microtubule assembly.

Localization of APC Protein at the Microtubule Plus Ends in Growing Axons

One downstream target of GSK-3β that is a potential regulator of axon microtubule assembly is APC. To localize APC in axons of embryonic DRG neurons, we stained the axons with an antibody recognizing the C terminus (Mimori-Kiyosue et al., 2000b). As shown in Figure 4A1, APC staining was intense in the soma and proximal axon, tapered off along the distal axon, and then was strikingly intense at the distal axon tip. Higher-magnification imaging showed that APC clustered at the very tip

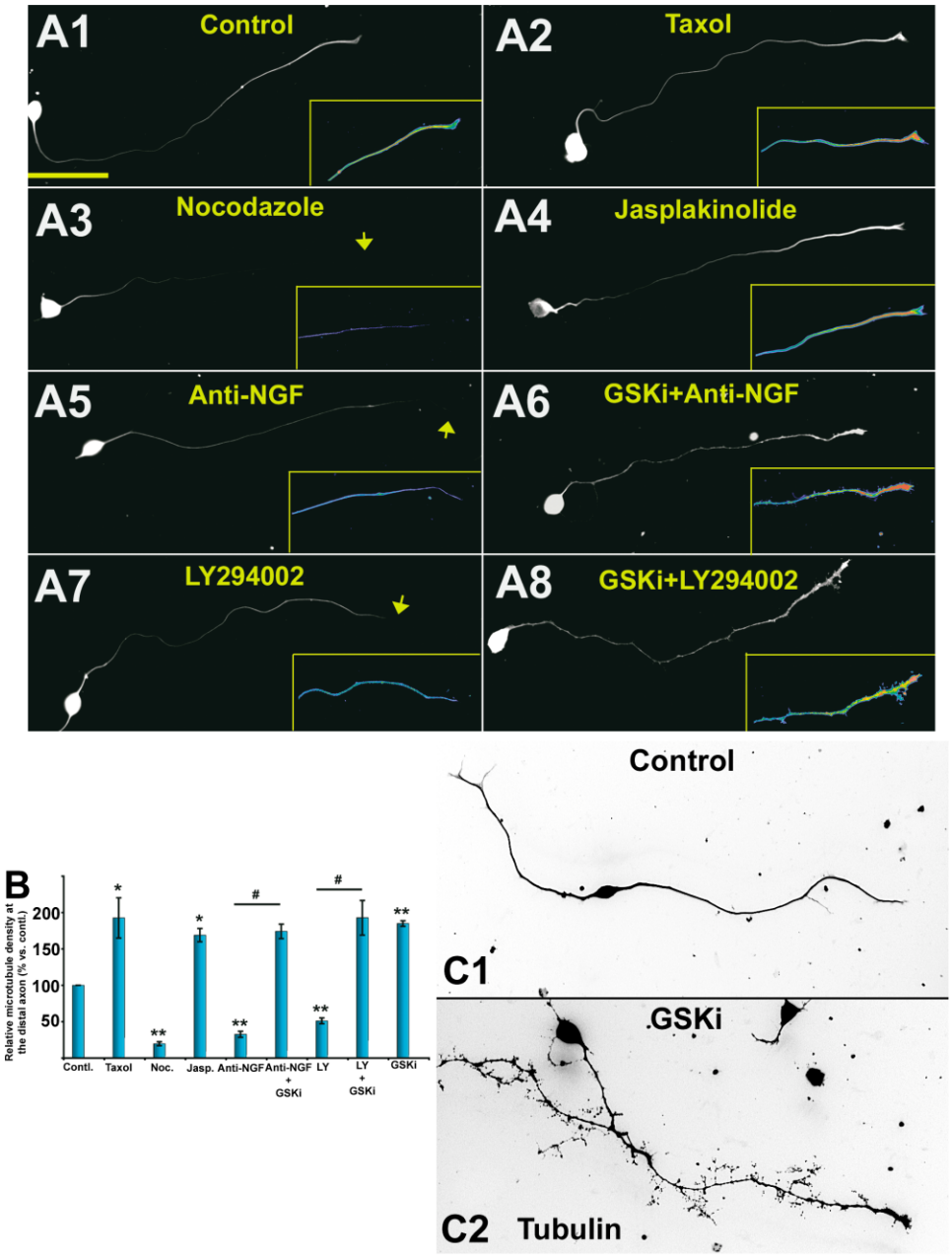

Figure 3. NGF Regulates Axonal Microtubule Levels during Axon Growth through the PI3K-GSK-3β Pathway

(A) Neurons were fixed and extracted at the same time to eliminate free tubulin monomers. Images in the insets were pseudocolored to indicate relative MT density at the distal axons. Red represents the highest fluorescent intensity and black indicates the lowest. In the control condition, polymerized microtubules (MT) showed a proximal-distal gradient distribution (A1). Taxol treatment significantly increased MT density, especially at the distal part of the axon (A2). Nocodazole treatment almost completely eliminated MT in the axon (A3). Retracted axons induced by jasplakinolide showed elevated MT density at the distal region (A4). Treatment of neurons with either anti-NGF or LY294002 resulted in decreased MT density at the distal axon (A5 and A7). This effect was antagonized completely by pretreatment with a specific GSK-3β inhibitor (A6 and A8).

(B) Quantification of relative MT density (compared to control axons) at the distal axon under each condition ($n = 3$ independent experiments, ANOVA, $p < 0.0001$). *$p < 0.05$, **$p < 0.001$ (versus control), #$p < 0.0001$ (between indicated groups).

(C) In control neurons, the axon shaft was smooth, indicating that MT were tightly bundled (C1). Inhibition of GSK-3β induced MT polymerization and axon branching along the entire axon shaft (C2).

of the microtubule bundles (Figure 4A2). Microtubules in these fast growing axons were highly bundled at their distal ends, and individual microtubule filaments were difficult to resolve. Thus, it was possible that the observed APC distribution could have been due to clustering of APC at the membrane near the microtubule ends rather than to direct binding of APC to the microtubules. To confirm that APC binds to microtubule plus ends,

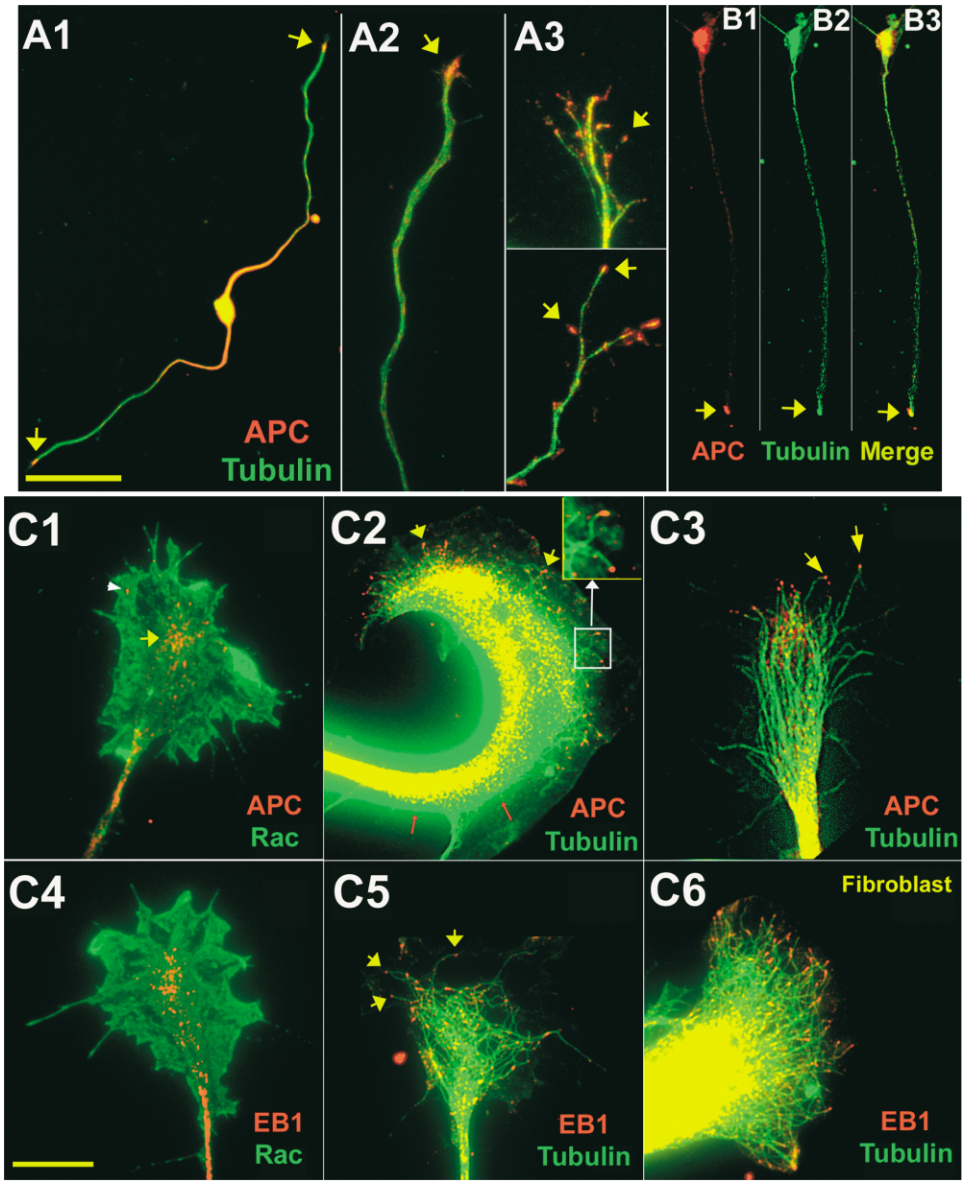

Figure 4. Localization of the APC Protein in Axons and Growth Cones of Mouse DRG Neurons

(A) Double immunofluorescence staining for tubulin and APC. APC staining was most intense at the soma, proximal axon, and distal tip ([A1], arrows). Higher-magnification imaging showed clustering of APC at the tip of the microtubule bundles ([A2], arrow). Axons treated with the actin depolymerization drug cytochalasin E had splayed microtubules, where APC was clearly seen decorating the tips of the single microtubules ([A3], arrows). Scale bar, 50 μm in (A1) and 16 μm in (A2) and (A3).

(B) APC staining at the axon tip was retained after neurons were extracted with Triton X-100 before fixation to eliminate cytosolic proteins ([B1], arrow). Microtubules at the axon tip that colocalized with APC were more resistant to detergent extraction ([B2 and B3], arrows).

(C) Overexpression of Rac was used to expand growth cones to allow precise APC localization. Within the growth cone, APC was mainly concentrated at the central domain, where most microtubules end (arrow). APC could also be observed in the actin-rich peripheral domain (white arrowhead). Double staining of APC and tubulin showed that APC localized to the distal tips of individual microtubules ([C2], arrows and inset) near the growth cone leading edge. Similar localization of APC at the microtubule tips was also observed in large control growth cones (C3). Another microtubule plus end binding protein, EB1, had a similar distribution to that of APC inside the growth cone (C4). Double staining showed that EB1 also localized at the tips of the single microtubules ([C5], arrows). As controls, EB1 was also present at the tips of individual microtubules in the fibroblasts (C6). Scale bar, 10 μm.

we treated neurons with cytochalasin to depolymerize actin filaments and therefore allow bundled microtubules at the axon tips to splay apart. After cytochalasin treatment, APC protein could be resolved as clearly decorating the tips of individual microtubules (Figure 4A3, arrows). To further confirm that APC binds to the microtubules, neurons were extracted with 1% Triton X-100 before fixation. As expected, APC was shown to be Triton X-100 insoluble, indicating cytoskeleton binding (Figures 4B1–4B3).

To directly visualize APC localization in control neurons without altering cytoskeletal structure, we trans-

fected neurons with wild-type Rac to obtain larger growth cones. These large growth cones displayed normal morphology and motility (data not shown) compared to the control growth cones. Microtubules in these Rac-expressing growth cones showed typical organization with most microtubules ending in the C domain and some individual dynamic microtubules protruding into the P domain. As shown in Figure 4C1, APC protein was mainly concentrated in the C domain of the growth cone, where most microtubules end (arrow). Some APC was also observed in the peripheral actin-rich region (arrowhead). Double staining for APC and tubulin revealed that some APC was clearly detected at the ends of individual dynamic microtubules (Figure 4C2, arrows and inset). This observation is consistent with previous studies in nonneuronal cells (Mimori-Kiyosue et al., 2000a) and indicates that APC indeed binds to the plus ends of microtubules in axons. Similar APC localization was also observed in large growth cones of neurons without Rac overexpression (Figure 4C3).

EB1 is another microtubule plus end binding protein that has been localized in axons (reviewed by Mimori-Kiyosue and Tsukita, 2003). When EB1 was stained in axons of DRG neurons, the protein showed a gradient distribution with higher intensity at the distal end (Supplemental Figure S2 at http://www.neuron.org/cgi/content/full/42/6/897/DC1). Higher-magnification imaging showed comet-like structures along the distal part of the axon (Supplemental Figure S2). The distribution of EB1 was different from the distribution of APC. EB1 distributes evenly along the distal region of the axon (Supplemental Figure S2), while APC accumulates at the very distal tip. In Rac-expressing neurons, EB1 had a similar distribution in the growth cone central domain to that of APC (Figures 4C4 and 4C5). As controls, fibroblasts in the same culture dish as DRG neurons were also examined for APC and EB1 staining. EB1 decorated the tips of all the polymerizing microtubules (Figure 4C6), while APC was not detected at the microtubule plus ends of fibroblasts (data not shown).

In nonneuronal cells, APC has been shown to bind to actin filaments as well as microtubules (Rosin-Arbesfeld et al., 2001). Double immunostaining of actin and APC in growth cones revealed that APC decorating the tips of dynamic microtubules tracked along actin bundles (Supplemental Figure S3A at http://www.neuron.org/cgi/content/full/42/6/897/DC1). This finding suggests APC as a potential mediator for interactions between dynamic microtubules and actin bundles (Zhou et al., 2002). Moreover, overexpressed C-terminal fragment of APC, C-APCΔMTB, which contains the EB1 binding motif and a putative PDZ binding domain, specifically accumulated as bundles in the peripheral domain of the growth cone where actin filaments are enriched (Supplemental Figure S3B).

Regulation of APC-Microtubule Interactions by the NGF-PI3K-GSK-3β Pathway

To ask whether NGF-PI3K-GSK-3β signaling regulates the APC-microtubule interaction at the axon tip, we tested the effects of various NGF signaling inhibitors on APC accumulation compared to controls (Figure 5A). Treatment with a function-blocking antibody against NGF for 1 hr induced growth cone collapse and dramatically diminished APC staining at the axon tips. This result indicates a regulatory role of NGF in APC accumulation. Two different PI3K inhibitors, LY294002 and wortmannin, caused growth cone collapse with decreased filamentous actin and significantly reduced APC accumulation. Similarly, the specific ILK inhibitor also induced growth cone collapse and decreased APC accumulation. An ERK inhibitor, U0126, however, had little effect on APC staining even though it induced similar growth cone collapse. Thus, ERK activation is not necessary for APC accumulation. This result also indicates that changes in actin organization (growth cone collapse) per se do not affect APC-microtubule interactions. This lack of dependence of APC accumulation on actin polymerization was confirmed by the result that the actin depolymerization reagent cytochalasin also had little effect on APC accumulation at the axon tips. All of these results are quantified in Figure 5B. Together, these results demonstrate that accumulation of APC at the microtubule plus ends in axons is regulated by the PI3K-ILK pathway downstream of NGF.

In nonneuronal cells, APC-microtubule interactions are regulated by phosphorylation. GSK-3β has been shown to phosphorylate APC and abolish its ability to bind to microtubules (Zumbrunn et al., 2001). As a result, diminished APC accumulation upon PI3K inhibition in axons could be due to the activation of GSK-3β. We therefore asked whether GSK-3β mediates the effect of PI3K in regulating APC-microtubule plus end association in axons. Treatment of neurons with a specific GSK-3β inhibitor completely prevented the loss of APC accumulation induced by the anti-NGF antibody, PI3K inhibitors, and the ILK inhibitor (Figures 5A and 5B), indicating that GSK-3β inhibition acts downstream of the NGF-PI3K-ILK pathway to mediate APC-microtubule interactions. Interestingly, GSK-3β inhibition did not fully rescue the growth cone collapsing effects of the NGF-PI3K pathway inhibitors, suggesting that GSK-3β may not mediate PI3K-dependent actin organization, which is also necessary for NGF-induced axon growth.

As shown in the preceding section, APC accumulation is mainly concentrated at the axon tips where GSK-3β is inactivated and is absent in the axon shaft where GSK-3β is active. When neurons were treated with GSK-3β inhibitors (lithium and GSK-3β inhibitor I) to directly inactivate GSK-3β along the entire length of the shaft, APC accumulation was observed along the entire length of the axon (Figure 5C). Moreover, this increased accumulation of APC along the axon shaft upon GSK-3β inhibition was well correlated with increased microtubule polymerization as shown above (Figure 5D). All of these results are consistent with the idea that inhibition of GSK-3β promotes microtubule assembly via increasing APC-microtubule interactions. Moreover, application of the GSK-3β inhibitor on axons separated from the cell bodies showed similar APC accumulation and microtubule assembly along the axon shafts, demonstrating that a local signaling cascade in the axon mediates these effects (Supplemental Figure S4).

Previous studies in nonneuronal cells have suggested that phosphorylation of GSK-3β via the PI3K pathway

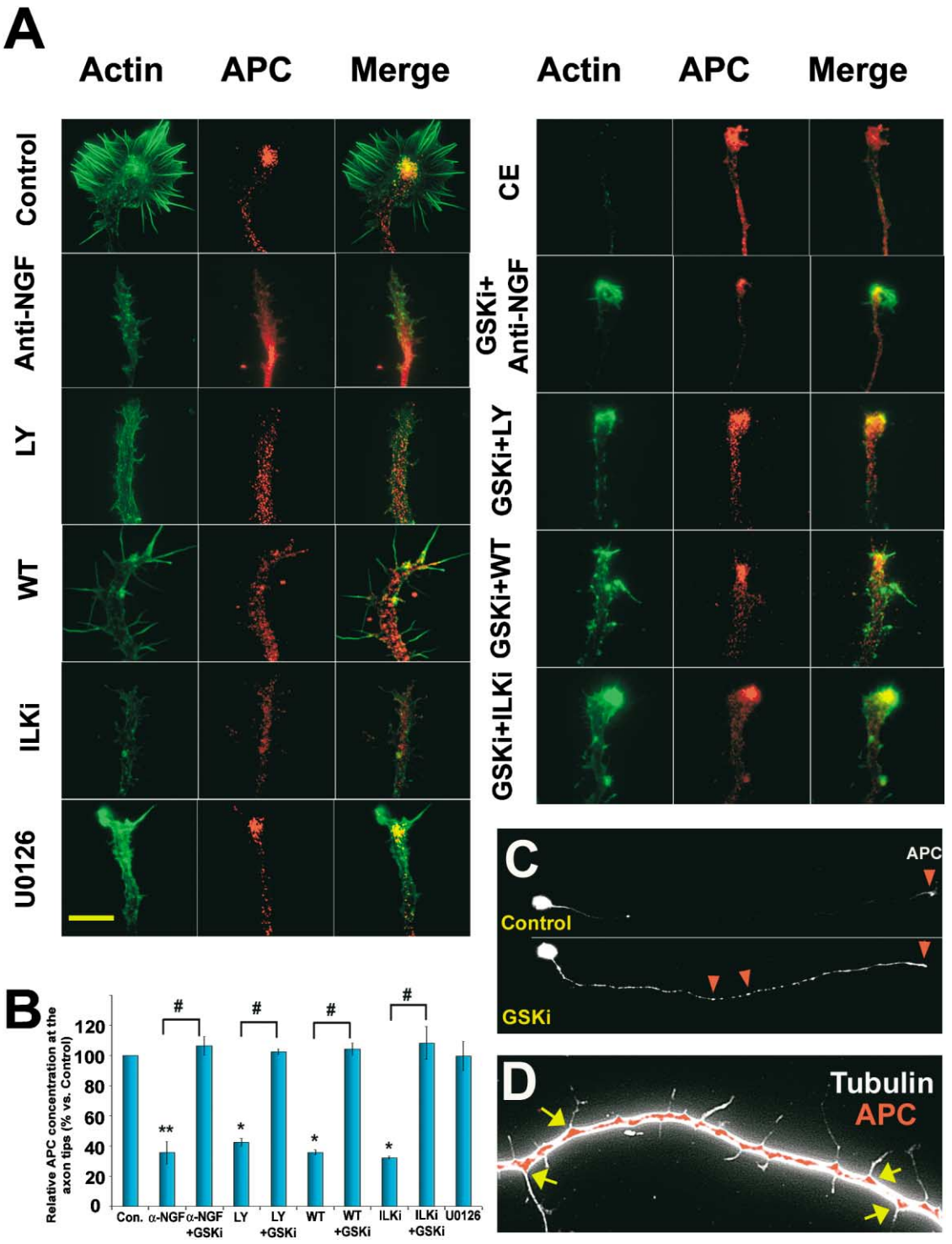

Figure 5. Regulation of APC-Microtubule Interactions by the NGF-PI3K-GSK-3β Pathway

(A) In control growth cones, APC accumulation was concentrated in the central domain. Actin depolymerization with cytochalasin E (CE) did not induce loss of APC staining. Treatment with anti-NGF caused growth cone collapse and eliminated the central domain APC accumulation. Two different PI3K inhibitors, LY294002 (LY) and wortmannin (WT), each induced similar growth cone collapse and loss of APC accumulation. A specific ILK inhibitor, KP-074728, also induced growth cone collapse and loss of APC accumulation. A specific ERK inhibitor, U0126, had little effect on APC accumulation even though it collapsed growth cone. Pretreatment of neurons with a specific GSK-3β inhibitor (GSKi) completely antagonized the effects of anti-NGF, LY, WT, and ILK inhibitor on APC accumulation. Scale bar, 10 μm.

(B) Quantification of APC accumulation at the axon tips ($n \geq 3$ independent experiments, ANOVA, $p < 0.0001$). * Represents a significant difference from control ($p < 0.0001$); ** represents $p < 0.01$; # represents a significant difference between indicated groups ($p < 0.0001$).

(C) In the control axon, APC accumulation was mainly detected at the tip of the axon (arrowhead), while little was observed in the axon shaft. Treatment with a GSK-3β inhibitor led to increased accumulation of APC along the axon shaft (arrowheads).

(D) In axons treated with a GSK-3β inhibitor, microtubule protrusions (white) were spatially correlated with APC accumulation (red) longitudinally along the axon. Note that the APC accumulations were also correlated with the direction of the microtubule protrusions transversally across the axon (arrows).

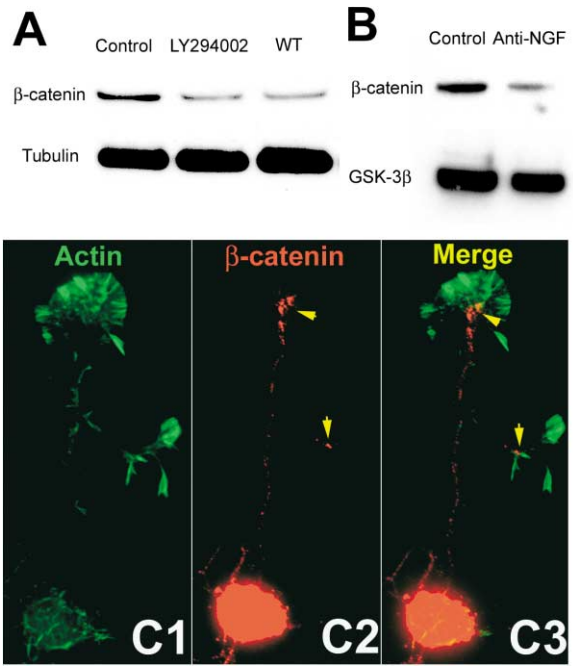

Figure 6. Regulation of β-Catenin by the NGF-PI3K Pathway

(A) Inhibition of PI3K activity with LY294002 or wortmannin induced significant decreases of total β-catenin protein level in axonal preparations. Similar results were obtained from three independent experiments.

(B) Withdrawal of NGF with anti-NGF antibody induced decreases of β-catenin protein in axons.

(C) Immunostaining showed localization of β-catenin at the tip of the axon (in the central domain of the growth cone, yellow arrows).

does not affect the β-catenin/APC complex in the Wnt pathway (see Cohen and Frame, 2001, for a review). However, more recently, phosphorylation of GSK-3β by PKCζ was shown to cause APC localization at microtubule plus ends in migrating astrocytes (Etienne-Manneville and Hall, 2003). To confirm that the NGF-PI3K pathway can access the β-catenin/APC complex in axons, we collected axons from cultured DRG neurons after anti-NGF antibody or PI3K inhibitor treatment. The results showed that both PI3K inhibitors and anti-NGF antibody induced loss of β-catenin protein in axons, likely due to activation of GSK-3β (Figures 6A and 6B). These results suggest that PI3K activation and GSK-3β phosphorylation protect β-catenin degradation in axons. Indeed, in growing axons, β-catenin is mainly concentrated at the tip of the axon, where GSK-3β is inactivated and APC accumulates (Figure 6C). Similar colocalization of β-catenin and APC at axon tips has been reported in cultured cortical neurons (Morrison et al., 1997). Together, our results establish that GSK-3β regulated by NGF-PI3K can influence β-catenin/APC.

Spatial Localization of APC at Distal Tips Is Necessary for Axon Growth Induced by NGF

To investigate the function of APC in regulating NGF-induced axon growth, we constructed a series of vectors expressing different functional domains of the protein fused to EGFP (Figure 7A). We first looked at the localization of these APC mutants in DRG neurons. N-terminal APC (N-APC) lacking the C-terminal microtubule and EB1 binding domains was only observed in the cell bodies and at the distal ends of the axon in the form of large aggregates (Figure 7B1). Higher-magnification imaging showed that the N-APC aggregates did not colocalize with individual microtubule plus ends (Figure 7B1, inset). This result indicates that the C-terminal microtubule binding domains of APC are not required for the anterograde transport of the APC protein along microtubules. Transport presumably occurs through binding to the motor protein kinesin via the N-terminal armadillo domain (Jimbo et al., 2002). Since N-APC also contains an oligomerization domain, overexpression of N-APC should therefore bind to the endogenous APC and interfere with its binding to the microtubules.

In contrast, C-terminal APC (C-APC) retaining both microtubule and EB1 binding domains but lacking other domains in the molecule was evenly distributed along the whole axon shaft (Figure 7B2). Moreover, there was no accumulation of C-APC at the distal end of the axon. C-terminal APC lacking the microtubule binding domain (C-APCΔMTB) can still bind to microtubules indirectly through an interaction with EB1 (Mimori-Kiyosue et al., 2000b). Expression of this construct showed a similar distal-proximal distribution along the axon to that of EB1 (Figure 7B3 versus Supplemental Figure S2 at http://www.neuron.org/cgi/content/full/42/6/897/DC1). Thus, C-APCΔMTB accumulated at the distal ends of the axons (Figure 7B3).

Analysis of axon growth showed that both N-APC and C-APC significantly retarded axon elongation induced by NGF (Figures 7D and 7E). Immunostaining with an antibody recognizing C-terminal APC revealed that endogenous APC was indeed associated with N-APC aggregates (Supplemental Figure S5A at http://www.neuron.org/cgi/content/full/42/6/897/DC1) and therefore presumably was prevented from binding to the microtubules and functioning properly. In contrast, C-APCΔMTB had little effect on axon growth (Figures 7D and 7E), probably because spatially distributed C-APCΔMTB by itself could stabilize microtubules together with endogenous EB1 protein (Nakamura et al., 2001). Our results are consistent with results reported by Green and Kaplan (2003). In that study, N-APC mutant protein similar to the one used here disrupted spindle microtubules during mitosis, while C-APCΔMTB had no effect.

To further confirm the functional role of APC in regulating axon growth, we generated a construct encoding the C-terminal fragment of EB1 (C-EB1), which lacks the microtubule binding domain but retains APC binding ability (Bu and Su, 2003). Overexpression of C-EB1 should therefore sequester endogenous APC and block its function. In support of this idea, Expressed C-EB1 was observed as large aggregates distributed along the axon (Figure 7C1) and colocalized with endogenous APC (Supplemental Figure S5B at http://www.neuron.org/cgi/content/full/42/6/897/DC1). We therefore tested C-EB1 in our axon growth assay. The result showed that expression of C-EB1 in DRG neurons markedly inhibited axon growth in the presence of NGF (Figures 7D and 7F). As a control, we made another C-EB1 construct

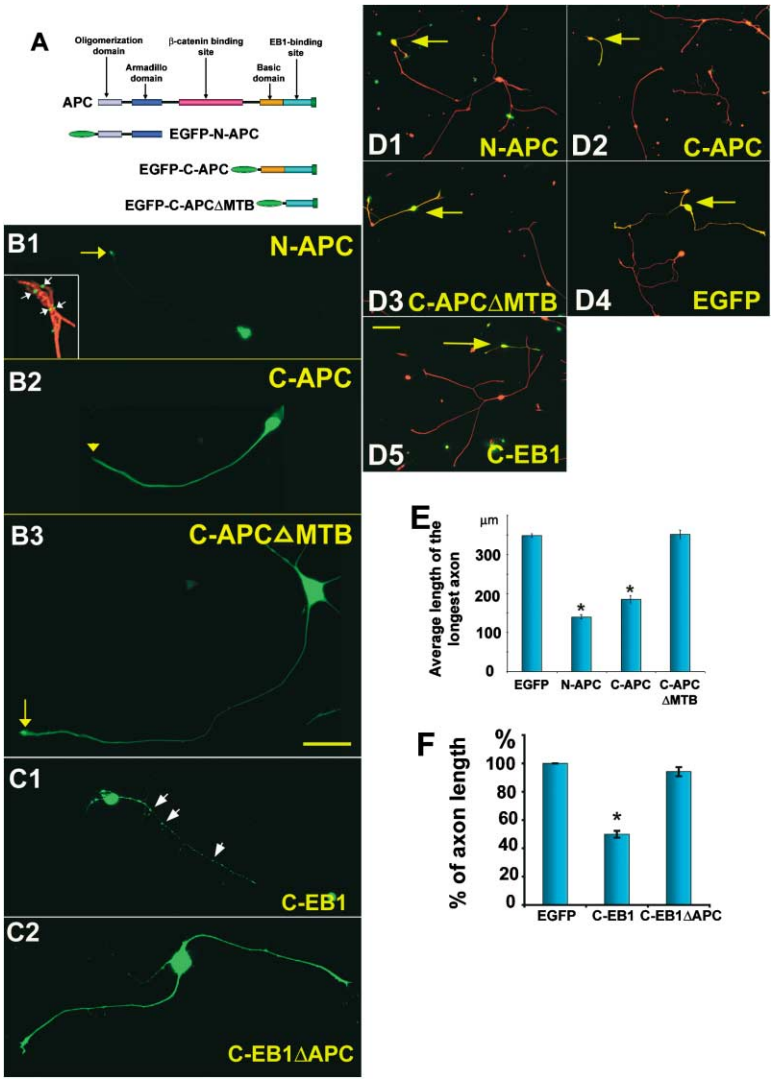

Figure 7. Functional Analysis of APC in Regulating NGF-Mediated Axon Elongation

(A) Schematic diagrams of the domain organization of APC and the three truncated mutant constructs used in the study.

(B) Localization of APC mutant proteins in the axon. N-APC (without microtubule binding domains) was mainly localized at the axon distal end ([B1], arrow) in the form of discrete aggregates (inset, white arrows) that did not bind to individual microtubule (red) tips. Expressed EGFP-C-APC distributed evenly along the axon without clear accumulation at the tip ([B2], arrow head). C-APC containing the EB1 binding domain but lacking the basic domain (EGFP-C-APCΔMTB) showed a gradient distribution along the axon with axon tip accumulation ([B3], arrow). Scale bar, 50 μm.

(C) Localization of EB1 mutant proteins in the axon. C-EB1 was distributed along the axon as large aggregates ([C1], white arrows). C-EB1ΔAPC distributed evenly along the axon (C2).

(D) Expression of N-APC (D1), C-APC (D2), and C-EB1 (D5) blocked axon growth compared to untransfected neurons or neurons expressing EGFP (D4). Expression of EGFP-C-APCΔMTB had little effect on axon growth (D3). Scale bar, 100 μm.

(E) Quantification of effects of different APC mutants on axon elongation (30 to 80 cells in three or more independent experiments were analyzed for each condition). * Indicates significant difference from the control ($p < 0.0001$).

(F) Quantification of effects of two EB1 mutants on axon growth. * Indicates significant difference from the control ($p < 0.0001$).

without the APC binding sequence (C-EB1ΔAPC). Expressed C-EB1ΔAPC distributed evenly along the axon similar to EGFP (Figure 7C2), and it had little effect on axon growth (Figure 7F). Together, these results indicate that sequestration of endogenous APC by C-EB1 blocks NGF-induced axon growth.

PI3K may regulate axonal microtubules either through stabilizing polymerized microtubules or through directly interfering with microtubule polymerization (the addition of tubulin monomers). To distinguish between the two possibilities, we examined EB1 localization as a marker for microtubule polymerization. Inhibition of PI3K with wortmannin had little effect on EB1 distribution along the axon (Supplemental Figure S2 at http://www.neuron.org/cgi/content/full/42/6/897/DC1), indicating that microtubule polymerization per se was not impeded by PI3K inhibition. This result also indicated that binding of EB1 to the microtubule plus ends did not depend on APC-microtubule interaction, consistent with previous studies (Mimori-Kiyosue et al., 2000b).

Potential Role of the GSK-3β-APC Pathway in Mediating Fast Axon Elongation

In addition to mediating NGF-induced axon growth, PI3K has been recently shown to be required for axon differentiation in cultured hippocampal neurons. Shi et al. (2003) have shown that PI3K is only activated at the tip of the axon, which is the fastest growing neurite. In order to assess GSK-3β activation in this setting, we stained stage 3 hippocampal neurons with anti-phospho-GSK-3β and showed that inactivated GSK-3β was concentrated at the tip of the axon, well correlated with PI3K activation (Figure 8A1). Strikingly, when APC was examined in these neurons, it accumulated only at the tips of the axon and not at the tips of dendrites (Figure 8A2). This result suggests that the GSK-3β-APC pathway may act downstream of PI3K and Par3/Par6/aPKC pathways in hippocampal neurons to regulate axon differentiation. Another example of fast axon elongation is injury-induced regenerative axon growth exhibited by adult peripheral neurons (Smith and Skene, 1997). We have

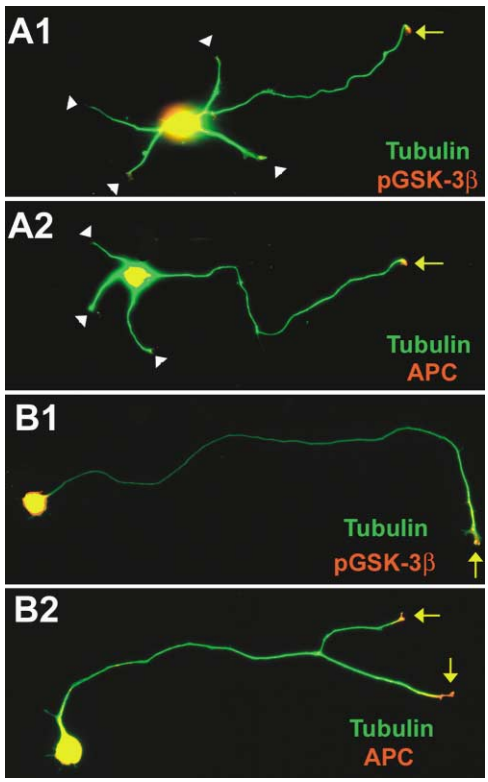

Figure 8. Localization of pGSK-3β and APC in Neurons with Rapidly Elongating Axons

(A) In embryonic hippocampal neurons, pGSk-3β was localized to the distal tip of the axon (yellow arrow) but not to the tips of dendrites ([A1], white arrowheads). Accordingly, APC only accumulated at the tip of the axon ([A2], yellow arrow).

(B) In mature regenerating DRG neurons, pGSK-3β was also localized to the distal tip (B1), colocalizing with APC accumulation (B2).

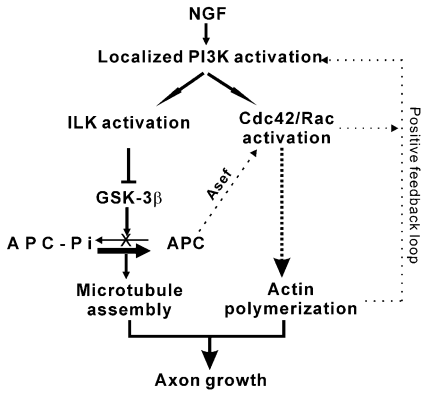

Figure 9. A Proposed Model for the Local NGF Signaling that Mediates Assembly of the Axonal Cytoskeleton

NGF activates PI3 kinase preferentially at the tip of the axon. Activated PI3K promotes actin polymerization at the growth cone leading edge via activation of the small GTPases Cdc42 and Rac. A positive feedback mechanism similar to that in migrating cells may underlie the spatial activation of PI3K at the axon tip in the face of uniform NGF stimulation. Spatially activated PI3K also induces a similarly localized inactivation of GSK-3β through ILK. Inactivation of GSK-3β allows the dephosphorylated APC protein to bind to the microtubule plus ends and therefore promotes microtubule assembly. Finally, microtubule polymerization at the plus ends together with APC may also affect actin dynamics through binding of APC to a Rac GTPase Exchange Factor (GEF), Asef.

previously shown that such regenerative axon elongation is NGF and PI3K independent (Liu and Snider, 2001). When axons of these regenerating neurons were examined, inactivation of GSK-3β and accumulation of APC were observed at the axon tips similar to the situation in embryonic neurons (Figure 8B). Taken together, our findings suggest that the GSK-3β-APC pathway may be accessed in growth cones of multiple classes of neurons and in DRG neurons by different upstream signaling pathways at different stages of development. The findings suggest that the GSK-3β-APC pathway may be a universal mediator in the control of microtubule assembly to achieve rapid axon growth.

Discussion

In this study, we have asked how NGF regulates axonal microtubules to mediate axon elongation. We demonstrate that PI3K activation downstream of NGF is localized to the growth cone and leads to similarly localized inactivation of GSK-3β. The localized GSK-3β inactivation at the growth cone then promotes efficient axon elongation via increasing the interactions between microtubules with the microtubule plus end binding protein APC. Our findings therefore demonstrate a novel pathway linking NGF signaling to a conserved cell polarization pathway that regulates microtubule dynamics at the growth cone. We suggest that NGF regulation of the GSK-3β-APC pathway at the growth cone underlies the ability of NGF to instruct rapid axon growth (Figure 9). We further suggest that this pathway affects microtubule dynamics relatively independently of actin filaments, which are often considered as the primary target of extracellular signals in growth cones (see Huber et al., 2003, for a review).

Spatial Regulation of the PI3K-GSK-3β Pathway by NGF Is Required for Efficient Axon Elongation

In this study, we have demonstrated that appropriate spatial localization of PI3K signaling is critical for efficient NGF-induced axon extension. The importance of localized PI3K signaling has also been demonstrated during directed cell migration. For example, during chemotaxis, PI3K is spatially activated at the leading edge of the migrating cells (see Iijima et al., 2002, for a review). Such polarized PI3K activation is correlated with localized actin polymerization, and both are necessary for directed cell migration (Wang et al., 2002). Suppression of PI3K activity with pharmacological inhibitors or dominant-negative constructs significantly blocked cell migration (Chung et al., 2001). Furthermore, recent findings have shown that cells expressing a membrane-targeted active PI3K or cells lacking the phosphatase PTEN that have unregulated PI3K activity also exhibited impaired migration upon chemoattractant stimulation (Funamoto et al., 2002). How this localized PI3K activity is generated

in axons in the presence of global NGF stimulation is unclear. One possibility is the involvement of a positive feedback loop involving PI3K signaling and actin (see Figure 9), as has been suggested to occur in neutrophils during chemotaxis (Weiner et al., 2002).

Similar to the situation for PI3K, GSK-3β was mainly inactivated at the growth cone, and indeed, inactive GSK-3β was almost perfectly colocalized with activated PI3K in the presence of NGF. Although the role of GSK-3β in regulating NGF-mediated axon growth has not previously been investigated, prior studies have identified GSK-3β as a downstream target of NGF-PI3K signaling in chicken DRG neurons (Eickholt et al., 2002) and in PC12 cells (Mills et al., 2003). Our data showed that, upon PI3K inhibition, some GSK-3β remained phosphorylated even though almost all Akt was inactivated (Figure 2). This result suggests that, in primary neurons, Akt may not mediate GSK-3β inactivation by PI3K as it does in other cell types (van Weeren et al., 1998). Another downstream target of PI3K, ILK, has been shown to phosphorylate GSK-3β downstream of NGF and PI3K in PC12 cells (Mills et al., 2003). Indeed, when ILK activity was inhibited, phosphorylation of GSK-3β was markedly decreased (Figure 2C), indicating that ILK acts downstream of PI3K to mediate GSK-3β inactivation in mouse DRG neurons.

It is important to emphasize that, in growing axons, microtubule polymerization is also spatially regulated. By comparing the amounts of polymerized microtubules under different experimental conditions, we found that inhibition of PI3K led to decreased microtubule levels, an effect that could be prevented by GSK-3β inhibition. These results identify PI3K and GSK-3β as mediators of NGF that regulate axonal microtubules in DRG neurons. The regulatory effect of PI3K and GSK-3β on axonal microtubule levels could be achieved through either affecting microtubule assembly or microtubule stabilization. Taken together, our findings demonstrate that two spatially coupled kinases are important in mediating NGF-induced axon elongation via the regulation of microtubules.

Functional Role of GSK-3β-APC Signaling in NGF-Induced Axon Growth

Despite its potential importance, the question of how microtubule binding proteins are regulated by neurotrophin signaling cascades has not previously been addressed (see Dent and Gertler, 2003). In addition to microtubule binding proteins that bundle and stabilize microtubules, such as MAP-1B and Tau (see below), there is a more recently identified group of microtubule plus end tracking proteins (+TIPs) (reviewed by Carvalho et al., 2003) that specifically bind to the polymerizing microtubule plus ends. These proteins regulate microtubule dynamics in nonneuronal cells during cell polarization processes (see Gundersen and Bretscher, 2003, for a review). In this study, we identify one of the +TIPs, APC, as a major microtubule binding protein that transduces neurotrophin signaling to axonal microtubule assembly. Our results demonstrate that APC binds to the plus ends of individual microtubules in the growth cone, suggesting an important role in regulating microtubule dynamics in neurons. It is well established that APC microtubule binding is abolished when APC is phosphorylated by GSK-3β (Zumbrunn et al., 2001). We show here that, in NGF-stimulated growing axons, APC molecules are spatially concentrated at growth cones, well correlated with the spatial distribution of GSK-3β inactivation. We therefore hypothesize that APC is part of the machinery that transduces spatially regulated PI3K-GSK-3β signaling to localized microtubule assembly.

How does APC regulate axonal microtubules during axon growth? Our results demonstrated that the loss of APC accumulation by inhibition of PI3K did not affect microtubule polymerization per se because there were no changes in EB1 staining, which acted as a marker for microtubule polymerization (Morrison et al., 2002). This result indicates that localized APC accumulation at the distal axon may not be required for microtubule polymerization (monomer addition). Thus the main function of APC at the growth cone may be to support microtubule stability, a well-characterized function in nonneuronal cells (Zumbrunn et al., 2001). Indeed, several lines of evidence in our study suggest that APC may play an important role in mediating microtubule-actin interactions in neurons, which have been suggested as one method of regulating microtubule stability in growth cones (reviewed by Zhou and Cohan, 2004).

MAP-1B and Tau are two other microtubule binding proteins that can be phosphorylated by GSK-3β. Interestingly, MAP-1B phosphorylation by GSK-3β is said to be independent of the serine 9 phosphorylation status of GSK-3β (Goold and Gordon-Weeks, 2001). NGF increases GSK-3β-mediated phosphorylation of MAP-1B in PC12 cells and sympathetic ganglion neurons (Goold and Gordon-Weeks, 2001). However, whether GSK-3β is the main kinase that regulates MAP-1B/microtubule interactions is unknown. Indeed, overexpression of GSK-3β in neuronal cell lines does not affect MAP-1B-microtubule binding (Goold et al., 1999). The major function of Tau is to bundle microtubules when it is dephosphorylated (Wagner et al., 1996), whereas in our study inhibition of GSK-3β induced microtubule debundling and polymerization along axon shafts. This result indicates that Tau is also unlikely to be a main target of GSK-3β in DRG neurons regulating microtubule assembly.

In addition to regulating axon growth, the GSK-3β-APC pathway may also control axon guidance if it is locally regulated by chemotropic or chemorepellant molecules. Indeed, both semaphorin 3A and Rho GTPase have been shown to regulate GSK-3β activity (Eickholt et al., 2002; Sayas et al., 2002). It would not be surprising if these guidance-signaling mediators were shown to regulate local microtubule dynamics directly via APC.

Cross-Talk between NGF Signaling and the GSK-3β-APC Pathway Locally in Axons

We report here that the GSK-3β-APC complex, normally considered a component of the Wnt pathway, can be accessed by neurotrophin signaling. Our result is thus in conflict with the current view that GSK-3β in the Wnt complex appears to be insulated from signaling triggered by receptor tyrosine kinases (see Cohen and Frame, 2001, for a review). The evidence for separation

of the pathways is that GSK-3β inhibited by insulin signaling does not result in β-catenin accumulation and that activation of Wnt signaling has no effect on glycogen synthase activity downstream of insulin signaling (Ding et al., 2000). How this compartmentalization is achieved and how broadly it applies is unclear. Interestingly, a recently published study showed that a cell polarity signaling complex, cdc42-par3/6-aPKC, could interact with the Wnt signaling pathway and regulate astrocyte migration via GSK-3β phosphorylation at serine 9 and APC binding to microtubule plus ends in astrocytes (Etienne-Manneville and Hall, 2003). In addition, ILK, a downstream target of PI3K, has also been shown to regulate β-catenin-Lef/Tcf-dependent transcription (Novak et al., 1998), and PTEN, a negative regulator of the PI3K pathway, can also regulate β-catenin-Lef/Tcf-dependent transcription involving phosphorylation of GSK-3β on serine 9 (Persad et al., 2001).

Our results provide evidence that NGF can also interact with Wnt downstream mediators and regulate APC phosphorylation through PI3K and ILK. The regulation of APC in axons via GSK-3β phosphorlation induced by PI3K signaling that we show here is similar in concept to these two previous examples of regulation of APC and β-catenin by phosphorylation of GSK-3β at serine 9. Additional evidence for the cross-talk between NGF signaling and Wnt mediators is provided by our finding that withdrawal of NGF or inhibition of PI3K led to a decreased level of β-catenin protein in axons. Several recent studies have documented roles for Wnt and β-catenin in axonal and dendritic branching (Krylova et al., 2002; Yu and Malenka, 2003). It is very likely that APC is involved in these processes via regulation of axonal microtubules. Based on our findings, it is tempting to hypothesize that Wnt and NGF may use the same machinery to control axon morphology. Through inhibition of GSK-3β, both Wnt and NGF can promote APC-microtubule interactions and at the same time stabilize β-catenin. Thus, coordinated microtubule assembly mediated by APC and cell adhesion mediated by β-catenin may regulate axon morphology. However, the final outcome (branching or elongation) is determined by the location of the signaling. NGF activates the GSK-3β-APC pathway at the distal axon and therefore promotes elongation, while Wnt activates it more proximally along the axon and induces branching. This idea is in line with findings from a recent study in which Wnt signaling has been shown to act as an attractive axon guidance cue when it is presented as a distal-proximal gradient (Lyuksyutova et al., 2003).

Implications In Vivo

Although several mouse mutants have been generated to address the roles of the GSK-3β and APC pathway, there is no clear view of the role of these molecules in vivo because of the possibility of "compensation" by family members. There are two isoforms of GSK-3, α and β. GSK-3β null mice have been reported to die at about embryonic day 13, mainly due to hepatocyte apoptosis, or at P1 due to respiratory difficulties and failure to feed (Hoeflich et al., 2000; Stankunas et al., 2003). However, before E-13 the *GSK-3*$\beta^{-/-}$ embryos showed no morphological abnormality, and cells from *GSK-3*$\beta^{-/-}$ mice had no defect in Wnt signaling (Hoeflich et al., 2000). These results suggest that the GSK-3 isoforms may compensate for each other in some situations but play distinct roles in others.

Most APC mutations result in truncated proteins lacking the C-terminal sequences that contain both the β-catenin and the microtubule binding domains (reviewed by Fearnhead et al., 2001). Mice that are homozygous for such APC mutations often die at early embryonic stages, preventing an analysis of the in vivo function of APC in axon growth. Another potential confounding factor in determining functions of APC in mouse genetic studies is the existence of an APC family member that may compensate for the functions of APC. Indeed, a nervous system-specific APC homolog, APC-L, has been identified (Nakagawa et al., 1998) and has been shown to regulate microtubule organization through the microtubule binding protein EB3 (Nakagawa et al., 2000). RT-PCR experiments have detected high-level expression of ALC-L in mouse DRG neurons (data not shown). Consistent with this idea, two APC homologs in *Drosophila*, APC1 and APC2, have been shown to play overlapping roles in regulating brain development (Akong et al., 2002). Altogether, it seems likely that the generation of mutant mice that are deficient in both APC family members specifically in the nervous system will be required to assess the role of APC proteins in regulating axon morphogenesis in vivo.

Experimental Procedures

Materials

A full list of pharmacological reagents, antibodies, and DNA constructs is provided in the Supplemental Data at http://www.neuron.org/cgi/content/full/42/6/897/DC1.

Gene Transfection and Pharmacology

DRG neurons were transfected with various DNA constructs using a newly developed transfection technique from Amaxa (Cologne, Germany). The transfection procedure was according to the Amaxa protocols for mouse neurons. Briefly, dissociated neurons were spun down to remove the supernatant completely and resuspended in 100 μl specified Amaxa electroporation buffer with 10–20 μg plasmid DNA. Suspended cells were then transferred to a 2.0 mm cuvette and electroporated with an Amaxa Nucleofector apparatus. After electroporation, cells were immediately transferred to the desired volume of culture medium and plated onto coated coverslips. After neurons fully attached to the substrates (2–4 hr), the medium was changed to remove the remnant transfection buffer. All the pharmacological inhibitors were added directly to the neuronal culture medium at indicated concentration and duration after overnight culture (20–24 hr). Cells were then fixed for further analysis. For each plasmid and pharmacological treatment, at least three independent experiments were conducted. Expression of N-APC and GSK-3β(S9A) frequently induced cell death. Therefore, we used neurons from *Bax* null mice or cotransfected a Bcl2 cDNA together with these constructs in the experiments.

Image Analysis and Statistics

All image analysis was done with Metamorph software. To measure axon length, the longest axon of each neuron was traced manually, and the length was then calculated. For experiments with high transfection efficiency (e.g., EGFP), about 50 neurons with axons were selected in each experiment. To achieve random sampling, the coverslips (eight for each experiment) were scanned using the CCD camera from the left to the right. The first 50 to 80 neurons encountered that had identifiable axons were recorded. For low transfection efficiency constructs (e.g., N-APC), all identifiable positive neurons with axons were selected for analysis.

To quantify the spatial distribution of Akt and GSK-3β activation, neurons were stained with phospho-Akt and phospho-GSK-3β, respectively, as well as a fluorescent dye, DTAF, that stains total protein (Schindelholz and Reber, 1999). Because cold methanol fixation disrupted the morphology of many growth cones in our culture, only ten neurons with positive pAkt staining from each experiment were selected for analysis. Twenty neurons with intact growth cones were chosen in each experiment for analysis of pGSK-3β staining (which did not require methanol fixation). The growth cone and a segment (about 50 μm) in the middle of the axon shaft were selected, and the average fluorescence intensity (AFI) of them from each channel was measured. The ratio of Akt or GSK-3β staining at the axon shaft versus at the growth cone was calculated and then normalized by the ratio of the DTAF staining.

To quantify APC localization at the tips of the axons, neurons were double stained with APC and phalloidin. In each independent experiment, 20 to 30 neurons from each experiment were selected and recorded at a 60× magnification with a CCD camera. For control experiments, the first 20 to 30 single neurons with intact and bright growth cones were selected. For experiments involving pharmacological inhibitors that caused growth cone collapse, only neurons with collapsed growth cones were chosen and recorded. A small region was created manually at the APC channel to outline the axon tip, and the AFI of this region was measured. The AFI of three randomly selected regions in the same image was also measured as background to obtain the adjusted AFI ($AFI_{axon\ tip} - AFI_{background}$) of APC staining. So that results from each independent experiment could be compared relative to one another, the mean of adjusted AFI from different conditions in each independent experiment was normalized by the control APC level and represented as a percentage value.

To quantify polymerized microtubules in the axon, neurons under various conditions were fixed and extracted at the same time and then stained with an anti-tubulin antibody. Fluorescence images were taken with a 20× objective. The distal region of the axon about 50 μm long was selected for microtubule density measurement according to the method described by He et al. (2002). Briefly, the total fluorescence intensity of the selected axon segment was measured. The background measurement was then subtracted to obtain the adjusted total fluorescence intensity. The final results were represented as average fluorescence intensity per micron length of axon.

All data were reported as mean ± SEM, and we used an unpaired Student's t test to determine the significance of the data between groups. "n" indicates the number of independent experiments. For multiple group comparison, one-way ANOVA was used, followed by t test as post hoc analysis.

See the Supplemental Data at http://www.neuron.org/cgi/content/full/42/6/897/DC1 for details of cell culture, Western blot analysis, and immunofluorescence studies.

Acknowledgments

We are grateful to Drs. Michal Hetman, Kun-ping Lu, Dianqing Wu, Lynne Cassimeris, and Mohanish Deshmukh for providing us with DNA constructs used in this study. We thank Drs. Patricia Maness, Franck Polleux, Jay Brenman, Tushar Patel, and Mark Walzer for helpful comments on the manuscript. This study is supported by a Spinal Cord Research Foundation fellowship (F.-Q.Z.) and NIH grant NS031768 (W.D.S.). Core 5 of an NINDS funded Center grant (P30 NS045892) was used to generate some of the images. The authors of this paper have declared a conflict of interest. For details, go to http://www.neuron.org/cgi/content/full/42/6/897/DC1.

Received: December 12, 2003
Revised: March 26, 2004
Accepted: May 10, 2004
Published: June 23, 2004

References

Akong, K., McCartney, B.M., and Peifer, M. (2002). Drosophila APC2 and APC1 have overlapping roles in the larval brain despite their distinct intracellular localizations. Dev. Biol. *250*, 71–90.

Atwal, J.K., Massie, B., Miller, F.D., and Kaplan, D.R. (2000). The TrkB-Shc site signals neuronal survival and local axon growth via MEK and P13-kinase. Neuron *27*, 265–277.

Baas, P.W., and Luo, L. (2001). Signaling at the growth cone: the scientific progeny of Cajal meet in Madrid. Neuron *32*, 981–984.

Bhat, R.V., Baraban, J.M., Johnson, R.C., Eipper, B.A., and Mains, R.E. (1994). High levels of expression of the tumor suppressor gene APC during development of the rat central nervous system. J. Neurosci. *14*, 3059–3071.

Brakeman, J.S., Gu, S.H., Wang, X.B., Dolin, G., and Baraban, J.M. (1999). Neuronal localization of the Adenomatous polyposis coli tumor suppressor protein. Neuroscience *91*, 661–672.

Bu, W., and Su, L.K. (2003). Characterization of functional domains of human EB1 family proteins. J. Biol. Chem. *278*, 49721–49731.

Campenot, R.B. (1982a). Development of sympathetic neurons in compartmentalized cultures. II. Local control of neurite survival by nerve growth factor. Dev. Biol. *93*, 13–21.

Campenot, R.B. (1982b). Development of sympathetic neurons in compartmentalized cultures. I. Local control of neurite growth by nerve growth factor. Dev. Biol. *93*, 1–12.

Cantley, L.C. (2002). The phosphoinositide 3-kinase pathway. Science *296*, 1655–1657.

Carvalho, P., Tirnauer, J.S., and Pellman, D. (2003). Surfing on microtubule ends. Trends Cell Biol. *13*, 229–237.

Chung, C.Y., Potikyan, G., and Firtel, R.A. (2001). Control of cell polarity and chemotaxis by Akt/PKB and PI3 kinase through the regulation of PAKa. Mol. Cell *7*, 937–947.

Cohen, P., and Frame, S. (2001). The renaissance of GSK3. Nat. Rev. Mol. Cell Biol. *2*, 769–776.

Cross, D.A., Alessi, D.R., Cohen, P., Andjelkovich, M., and Hemmings, B.A. (1995). Inhibition of glycogen synthase kinase-3 by insulin mediated by protein kinase B. Nature *378*, 785–789.

Crowder, R.J., and Freeman, R.S. (2000). Glycogen synthase kinase-3 beta activity is critical for neuronal death caused by inhibiting phosphatidylinositol 3-kinase or Akt but not for death caused by nerve growth factor withdrawal. J. Biol. Chem. *275*, 34266–34271.

Dent, E.W., and Gertler, F.B. (2003). Cytoskeletal dynamics and transport in growth cone motility and axon guidance. Neuron *40*, 209–227.

Ding, V.W., Chen, R.H., and McCormick, F. (2000). Differential regulation of glycogen synthase kinase 3beta by insulin and Wnt signaling. J. Biol. Chem. *275*, 32475–32481.

Eickholt, B.J., Walsh, F.S., and Doherty, P. (2002). An inactive pool of GSK-3 at the leading edge of growth cones is implicated in Semaphorin 3A signaling. J. Cell Biol. *157*, 211–217.

Etienne-Manneville, S., and Hall, A. (2003). Cdc42 regulates GSK-3beta and adenomatous polyposis coli to control cell polarity. Nature *421*, 753–756.

Fearnhead, N.S., Britton, M.P., and Bodmer, W.F. (2001). The ABC of APC. Hum. Mol. Genet. *10*, 721–733.

Funamoto, S., Meili, R., Lee, S., Parry, L., and Firtel, R.A. (2002). Spatial and temporal regulation of 3-phosphoinositides by PI 3-kinase and PTEN mediates chemotaxis. Cell *109*, 611–623.

Gallo, G., and Letourneau, P.C. (1998). Localized sources of neurotrophins initiate axon collateral sprouting. J. Neurosci. *18*, 5403–5414.

Gallo, G., Yee, H.F., Jr., and Letourneau, P.C. (2002). Actin turnover is required to prevent axon retraction driven by endogenous actomyosin contractility. J. Cell Biol. *158*, 1219–1228.

Goold, R.G., and Gordon-Weeks, P.R. (2001). Microtubule-associated protein 1B phosphorylation by glycogen synthase kinase 3beta is induced during PC12 cell differentiation. J. Cell Sci. *114*, 4273–4284.

Goold, R.G., Owen, R., and Gordon-Weeks, P.R. (1999). Glycogen synthase kinase 3beta phosphorylation of microtubule-associated protein 1B regulates the stability of microtubules in growth cones. J. Cell Sci. *112*, 3373–3384.

Gordon-Weeks, P.R. (1991). Growth cones: the mechanism of neurite advance. Bioessays *13*, 235–239.

Green, R.A., and Kaplan, K.B. (2003). Chromosome instability in colorectal tumor cells is associated with defects in microtubule plus-end attachments caused by a dominant mutation in APC. J. Cell Biol. *163*, 949–961.

Gundersen, G.G., and Bretscher, A. (2003). Cell biology. Microtubule asymmetry. Science *300*, 2040–2041.

He, Y., Yu, W., and Baas, P.W. (2002). Microtubule reconfiguration during axonal retraction induced by nitric oxide. J. Neurosci. *22*, 5982–5991.

Hetman, M., Cavanaugh, J.E., Kimelman, D., and Xia, Z. (2000). Role of glycogen synthase kinase-3beta in neuronal apoptosis induced by trophic withdrawal. J. Neurosci. *20*, 2567–2574.

Hoeflich, K.P., Luo, J., Rubie, E.A., Tsao, M.S., Jin, O., and Woodgett, J.R. (2000). Requirement for glycogen synthase kinase-3beta in cell survival and NF-kappaB activation. Nature *406*, 86–90.

Huber, A.B., Kolodkin, A.L., Ginty, D.D., and Cloutier, J.F. (2003). Signaling at the growth cone: ligand-receptor complexes and the control of axon growth and guidance. Annu. Rev. Neurosci. *26*, 509–563.

Iijima, M., Huang, Y.E., and Devreotes, P. (2002). Temporal and spatial regulation of chemotaxis. Dev. Cell *3*, 469–478.

Jimbo, T., Kawasaki, Y., Koyama, R., Sato, R., Takada, S., Haraguchi, K., and Akiyama, T. (2002). Identification of a link between the tumour suppressor APC and the kinesin superfamily. Nat. Cell Biol. *4*, 323–327.

Kanzaki, M., Mora, S., Hwang, J.B., Saltiel, A.R., and Pessin, J.E. (2004). Atypical protein kinase C (PKC{zeta}/{lambda}) is a convergent downstream target of the insulin-stimulated phosphatidylinositol 3-kinase and TC10 signaling pathways. J. Cell Biol. *164*, 279–290.

Krylova, O., Herreros, J., Cleverley, K.E., Ehler, E., Henriquez, J.P., Hughes, S.M., and Salinas, P.C. (2002). WNT-3, expressed by motoneurons, regulates terminal arborization of neurotrophin-3-responsive spinal sensory neurons. Neuron *35*, 1043–1056.

Liu, R.Y., and Snider, W.D. (2001). Different signaling pathways mediate regenerative versus developmental sensory axon growth. J. Neurosci. *21*, RC164.

Lyuksyutova, A.I., Lu, C.C., Milanesio, N., King, L.A., Guo, N., Wang, Y., Nathans, J., Tessier-Lavigne, M., and Zou, Y. (2003). Anterior-posterior guidance of commissural axons by Wnt-frizzled signaling. Science *302*, 1984–1988.

Markus, A., Patel, T.D., and Snider, W.D. (2002a). Neurotrophic factors and axonal growth. Curr. Opin. Neurobiol. *12*, 523–531.

Markus, A., Zhong, J., and Snider, W.D. (2002b). Raf and akt mediate distinct aspects of sensory axon growth. Neuron *35*, 65–76.

Mills, J., Digicaylioglu, M., Legg, A.T., Young, C.E., Young, S.S., Barr, A.M., Fletcher, L., O'Connor, T.P., and Dedhar, S. (2003). Role of integrin-linked kinase in nerve growth factor-stimulated neurite outgrowth. J. Neurosci. *23*, 1638–1648.

Mimori-Kiyosue, Y., and Tsukita, S. (2001). Where is APC going? J. Cell Biol. *154*, 1105–1109.

Mimori-Kiyosue, Y., and Tsukita, S. (2003). "Search-and-Capture" of microtubules through plus-end-binding proteins (+TIPs). J. Biochem. (Tokyo) *134*, 321–326.

Mimori-Kiyosue, Y., Shiina, N., and Tsukita, S. (2000a). Adenomatous polyposis coli (APC) protein moves along microtubules and concentrates at their growing ends in epithelial cells. J. Cell Biol. *148*, 505–518.

Mimori-Kiyosue, Y., Shiina, N., and Tsukita, S. (2000b). The dynamic behavior of the APC-binding protein EB1 on the distal ends of microtubules. Curr. Biol. *10*, 865–868.

Ming, G., Song, H., Berninger, B., Inagaki, N., Tessier-Lavigne, M., and Poo, M. (1999). Phospholipase C-gamma and phosphoinositide 3-kinase mediate cytoplasmic signaling in nerve growth cone guidance. Neuron *23*, 139–148.

Morrison, E.E., Askham, J., Clissold, P., Markham, A.F., and Meredith, D.M. (1997). Expression of beta-catenin and the adenomatous polyposis coli tumour suppressor protein in mouse neocortical cells in vitro. Neurosci. Lett. *235*, 129–132.

Morrison, E.E., Moncur, P.M., and Askham, J.M. (2002). EB1 identifies sites of microtubule polymerisation during neurite development. Brain Res. Mol. Brain Res. *98*, 145–152.

Nakagawa, H., Murata, Y., Koyama, K., Fujiyama, A., Miyoshi, Y., Monden, M., Akiyama, T., and Nakamura, Y. (1998). Identification of a brain-specific APC homologue, APCL, and its interaction with beta-catenin. Cancer Res. *58*, 5176–5181.

Nakagawa, H., Koyama, K., Murata, Y., Morito, M., Akiyama, T., and Nakamura, Y. (2000). EB3, a novel member of the EB1 family preferentially expressed in the central nervous system, binds to a CNS-specific APC homologue. Oncogene *19*, 210–216.

Nakamura, M., Zhou, X.Z., and Lu, K.P. (2001). Critical role for the EB1 and APC interaction in the regulation of microtubule polymerization. Curr. Biol. *11*, 1062–1067.

Novak, A., Hsu, S.C., Leung-Hagesteijn, C., Radeva, G., Papkoff, J., Montesano, R., Roskelley, C., Grosschedl, R., and Dedhar, S. (1998). Cell adhesion and the integrin-linked kinase regulate the LEF-1 and beta-catenin signaling pathways. Proc. Natl. Acad. Sci. USA *95*, 4374–4379.

Persad, S., Troussard, A.A., McPhee, T.R., Mulholland, D.J., and Dedhar, S. (2001). Tumor suppressor PTEN inhibits nuclear accumulation of beta-catenin and T cell/lymphoid enhancer factor 1-mediated transcriptional activation. J. Cell Biol. *153*, 1161–1174.

Reif, K., Nobes, C.D., Thomas, G., Hall, A., and Cantrell, D.A. (1996). Phosphatidylinositol 3-kinase signals activate a selective subset of Rac/Rho-dependent effector pathways. Curr. Biol. *6*, 1445–1455.

Rosin-Arbesfeld, R., Ihrke, G., and Bienz, M. (2001). Actin-dependent membrane association of the APC tumour suppressor in polarized mammalian epithelial cells. EMBO J. *20*, 5929–5939.

Sayas, C.L., Avila, J., and Wandosell, F. (2002). Glycogen synthase kinase-3 is activated in neuronal cells by Galpha12 and Galpha13 by Rho-independent and Rho-dependent mechanisms. J. Neurosci. *22*, 6863–6875.

Schindelholz, B., and Reber, B.F. (1999). Quantitative estimation of F-actin in single growth cones. Methods *18*, 487–492.

Segal, R.A. (2003). Selectivity in neurotrophin signaling: theme and variations. Annu. Rev. Neurosci. *26*, 299–330.

Shi, S.H., Jan, L.Y., and Jan, Y.N. (2003). Hippocampal neuronal polarity specified by spatially localized mPar3/mPar6 and PI 3-kinase activity. Cell *112*, 63–75.

Smith, D.S., and Skene, J.H. (1997). A transcription-dependent switch controls competence of adult neurons for distinct modes of axon growth. J. Neurosci. *17*, 646–658.

Stankunas, K., Bayle, J.H., Gestwicki, J.E., Lin, Y.M., Wandless, T.J., and Crabtree, G.R. (2003). Conditional protein alleles using knockin mice and a chemical inducer of dimerization. Mol. Cell *12*, 1615–1624.

Sutherland, C., Leighton, I.A., and Cohen, P. (1993). Inactivation of glycogen synthase kinase-3 beta by phosphorylation: new kinase connections in insulin and growth-factor signalling. Biochem. J. *296*, 15–19.

Thomas, G.M., Frame, S., Goedert, M., Nathke, I., Polakis, P., and Cohen, P. (1999). A GSK3-binding peptide from FRAT1 selectively inhibits the GSK3-catalysed phosphorylation of axin and beta-catenin. FEBS Lett. *458*, 247–251.

van Weeren, P.C., de Bruyn, K.M., de Vries-Smits, A.M., van Lint, J., and Burgering, B.M. (1998). Essential role for protein kinase B (PKB) in insulin-induced glycogen synthase kinase 3 inactivation. Characterization of dominant-negative mutant of PKB. J. Biol. Chem. *273*, 13150–13156.

Wagner, U., Utton, M., Gallo, J.M., and Miller, C.C. (1996). Cellular phosphorylation of tau by GSK-3 beta influences tau binding to microtubules and microtubule organisation. J. Cell Sci. *109*, 1537–1543.

Wang, F., Herzmark, P., Weiner, O.D., Srinivasan, S., Servant, G., and Bourne, H.R. (2002). Lipid products of PI(3)Ks maintain persis-

tent cell polarity and directed motility in neutrophils. Nat. Cell Biol. *4*, 513–518.

Weiner, O.D., Neilsen, P.O., Prestwich, G.D., Kirschner, M.W., Cantley, L.C., and Bourne, H.R. (2002). A PtdInsP(3)- and Rho GTPase-mediated positive feedback loop regulates neutrophil polarity. Nat. Cell Biol. *4*, 509–513.

Woodgett, J.R. (2001). Judging a protein by more than its name: GSK-3. Sci. STKE, RE12.

Yu, X., and Malenka, R.C. (2003). beta-catenin is critical for dendritic morphogenesis. Nat. Neurosci. *6*, 1169–1177.

Zhou, F.Q., and Cohan, C.S. (2004). How actin filaments and microtubules steer growth cones to their targets. J. Neurobiol. *58*, 84–91.

Zhou, F.Q., Waterman-Storer, C.M., and Cohan, C.S. (2002). Focal loss of actin bundles causes microtubule redistribution and growth cone turning. J. Cell Biol. *157*, 839–849.

Zumbrunn, J., Kinoshita, K., Hyman, A.A., and Nathke, I.S. (2001). Binding of the adenomatous polyposis coli protein to microtubules increases microtubule stability and is regulated by GSK3 beta phosphorylation. Curr. Biol. *11*, 44–49.